HHS Public Access

Author manuscript

J Biomed Mater Res B Appl Biomater. Author manuscript; available in PMC 2015 June 29.

Published in final edited form as:

J Biomed Mater Res B Appl Biomater. 2014 November ; 102(8): 1779–1785. doi:10.1002/jbm.b.33167.

Local mechanical response of cells to the controlled rotation of magnetic nanorods

Matias Castillo[1], **Roberto Ebensperger**[2], **Denis Wirtz**[3,4,5], **Magdalena Walczak**[1], **Daniel E. Hurtado**[6,*], and **Alfredo Celedon**[1,7,*]

[1]Department of Mechanical and Metallurgical Engineering, Pontificia Universidad Católica de Chile, Vicuña Mackenna 4860, Macul, Santiago, Chile

[2]Department of Pharmacy, Pontificia Universidad Católica de Chile, Vicuña Mackenna 4860, Macul, Santiago, Chile

[3]Department of Chemical and Biomolecular Engineering, The Johns Hopkins University, Baltimore, Maryland 21218

[4]Johns Hopkins Physical Sciences–Oncology Center, The Johns Hopkins University, Baltimore, Maryland 21218

[5]Departments of Oncology and Pathology and Sidney Kimmel Comprehensive Cancer Center, The Johns Hopkins University School of Medicine, Baltimore, Maryland 21205

[6]Department of Structural and Geotechnical Engineering, Pontificia Universidad Católica de Chile, Vicuña Mackenna 4860, Macul, Santiago, Chile

[7]Institute for NanoBiotechnology, The Johns Hopkins University, Baltimore, Maryland 21218

Abstract

The mechanical response of the cytoplasm was investigated by the intracellular implantation of magnetic nanorods and exposure to low-frequency rotatory magnetic fields. Nanorods (Pt-Ni, ~200 nm diameter) fabricated by electrodeposition in templates of porous alumina with lengths of approximately 2 and 5 μm were inserted into NIH/ 3T3 fibroblasts and manipulated with a rotational magnetic field. Nanorod rotation was observed only for torques greater than 3.0×10^{-16} Nm, suggesting a Bingham-type behavior of the cytoplasm. Higher torques produced considerable deformation of the intracellular material. The cell nucleus and cell membrane were significantly deformed by nanorods actuated by 4.5×10^{-15} Nm torques. Our results demonstrate that nanorods under magnetic fields are an effective tool to mechanically probe the intracellular environment. We envision that our findings may contribute to the noninvasive and direct mechanical characterization of the cytoplasm.

Keywords

magnetic nanorods; rotatory magnetic field; cytoplasm mechanics; Bingham fluid

Correspondence to: D. E. Hurtado (dhurtado@ing.puc.cl) or A. Celedon (aceledon@ing.puc.cl).

INTRODUCTION

Magnetic nanoparticles are a promising tool for biological and therapeutic applications such as tumor ablation,[1] drug delivery,[2] and magnetic resonance diagnostics.[3] Their low dimensions allow simple insertion into cells[4] and controlled interaction with cellular proteins,[5,6] whereas their magnetic properties enable noninvasive and highly localized mechanical manipulation using external magnetic fields without compromising the surrounding tissues.

The intracellular behavior of magnetic spherical nanoparticles (~20 nm radius) has been recently investigated in cellular destruction studies,[7,8] where high-frequency magnetic fields in the range of kHz to MHz induce hyperthermia mainly by Néel's relaxation,[9] that is, inducing fluctuations of the particle's magnetic moment that ultimately release heat to the surrounding tissue. The cytoplasm rheology has been studied using magnetic spheres that self-assemble into elongated structures that undergo partial rotations and small-amplitude oscillations under a low-frequency (Hz) magnetic field.[10] Nanorods (~200 nm diameter, ~1–10 μm length) implanted in NIH 3T3 fibroblast cultures have also been exposed to low-frequency (1 Hz) magnetic fields.[11] These studies concentrate on the cellular destruction caused by large aggregates of nanoparticles that mechanically disrupt the cellular environment. All the investigations just described focus on small levels of mechanical deformation, but larger amplitudes of particle rotation, including full rotation, and larger amount of deformation of intracellular structures has not been investigated to date.

The ability of probing the mechanical characteristics of cellular structures is essential to understand cell function, as mechanical stimuli directly affects the biochemical and biological behavior of the cell.[12] In a previous work,[13] we studied the microrheological properties of the nucleus. Nanorods were inserted by ballistic injection into the nucleus and later exposed to magnetic field to align nanorods. The magnetic field was rotated by 90° and the response of nanorod over time was analyzed. In this work, we passively introduce nanorods inside cells and investigate the extent to which individual platinum–nickel nanorods subjected to rotatory low-frequency magnetic fields can deform cell structures in the cytoplasm, as well as the plasma and nuclear membranes, together with determining the magnetic-induced torque level that triggers intracellular mechanical deformation.

MATERIALS AND METHODS

Nanorod fabrication

Pt–Ni nanorods [Figure 1(a)] were fabricated by electrochemical deposition in the pores of anodized aluminum oxide (AAO) membranes (Whatman, Springfield Mill, Kent, UK).[14] AAO templates were sputtered with a 150 nm copper layer to block the nanopores and to act as the cathode in subsequent electrodeposition. Negative potential sequences were used to generate the current required to deposit the different metal electrolyte solutions. The first deposition was a sacrificial segment of Cu obtained from a copper sulfate solution (0.5 M $CuSO_4 \cdot 5H_2O$, pH=1.0). Then, the Pt segment (nonmagnetic) was deposited from an ammonium hexachloroplatinate solution (17 mM $(NH_4)_2PtCl_6$ and 250 mM Na_2HPO_4, pH=7.8). The Ni deposition from a Ni sulfate solution (0.5 M $NiSO_4 \cdot 6H_2O$ and 0.67 M

H_3BO_3, pH=3.8) determined the strength of the magnetic dipole of the nanorods. The time of application of the electrical current was determined from fabrication protocols to obtain the desired length of the metallic segment. To remove the copper layer, the templates were submerged in a copper etchant bath, BTP (Transene, Danvers, MA), for 13 h at 40°C. Similarly, the oxide membranes were removed in an 11 h bath of 2 M KOH at 65°C. The released nanorods were finally sonicated to ensure dispersion and subsequently suspended in ethanol for storage.

Two types of nanorods were targeted during fabrication: 5 μm-long nanorods with a Pt/Ni ratio of 4:1 and 2 μm-long nanorods with a Pt/Ni ratio of 1:1. Both types of nanorods had a 1-μm -longnickel segment. The diameter of the nanorods was defined by the nominal diameter of the templates pores (~200 nm). The uniformity of various nanorod preparations was analyzed using scanning-electron (SEM) and bright-field microscopy. The two different sizes of the platinum segment allowed us to study the effect of size on the mobility of the nanorods inside the cells. It also helped avoid nanorod agglomeration and facilitate quantitative analysis of their movements with high temporal and spatial resolutions.

Cell culture and insertion of nanorods

NIH/3T3 mouse fibroblasts were cultured in polystyrene Petri dishes in Dulbecco's modified Eagle's medium (DMEM) with high glucose, complemented with 1% antibiotics and 10% fetal bovine serum. The cells where maintained in a 5% CO_2 humidified atmosphere at 37°C. The cells were passaged and the growth medium was renewed for every 3 days.

Cells were deposited onto 9 mm-diameter silicon wells (60 μL each) with an initial average density of 4000 cells per well. The samples were incubated for 24 h in the growth environment to obtain firm cell–cell and cell–matrix adhesion and high confluence. Groups of approximately 5 and 2 μm length nanorods were separated from ethanol and suspended in DMEM, obtaining an estimated average nanorod concentration of 0.42 and 0.14 μg/mL for the 5- and 2-μm solutions, respectively. The resulting magnetic fluid was sonicated to avoid rod agglomeration and deposited immediately in the wells containing the cells for which the DMEM was previously removed. The samples were incubated for another 24 h to allow for the insertion of nanorods into the cells.

The internalization of nanorods of similar dimensions in NIH/3T3 cells has been demonstrated by cross-sectional reconstruction of fibroblast[11] and by analyzing their Brownian motions.[15]

Generation and operation of the rotatory magnetic field

A set-up of two 25 × 25 × 10 mm^3 cube-shaped neodymium- iron-boron (NdFeB) permanent magnets separated by a gap of 3 mm was mounted on top of a petri dish and was coaxially rotated to generate a rotatory magnetic field [Figure 1(b)]. The vertical distance between the petri dish and magnets was manually tuned to achieve the desired magnetic intensity. To maximize the field intensity at the experimental probes location, a vertical antiparallel orientation of the magnets was used, with two iron blocks connecting the upper faces of the magnets to suppress and guide the magnetic flux [Figure 1(b)]. This

configuration generates a horizontal magnetic field in the central vertical axis below the magnets [Figure 1(c)]. To rotate the horizontal field, the magnets were fixed on an angular contact ball-bearing system, and connected by gears to a D.C. generator for speed control.

For different vertical separation, we measured the magnetic field intensity at the sample using a 4048 Gauss/Tesla Meter (F.W. Bell) [Figure 1(d)]. We obtained a maximum of 890 mT for a separation of 5 mm from the magnet's midplane to the magnet's bottom surface.

Application of controlled torque on nanorods

To study the effect of the magnetic field intensity on the nanorod rotation, a single revolution of the magnetic field with a total duration of 20 s was applied over the sample. Digital images of a region of the sample containing at least 3 cells with embedded nanorods were acquired using an optical inverted microscope (Motic, AE2000) at an average rate of 2 s per frame. Magnetic-field intensities of 20, 60, 140, and 300 mT were generated by regulating the distance between the magnet and the sample [Figure 1(d)]. A total of 20 nanorods were studied from the digital images for which the orientation was manually determined. After testing, the samples were discarded.

To analyze the long-term mechanical behavior of the nanorods, a rotatory magnetic field with a frequency of 10 Hz and an intensity of 300 mT was applied to each sample for 10 min, after which digital images were acquired in a few seconds. Four subsequent cycles were completed in each test, with a total duration of 40 min. A total of 23 nanorods were studied from the digital images, for which the orientation was manually determined.

RESULTS

Dimensions and subcellular location of magnetic nanorods

The dimensions of nanorods were measured from SEM images, resulting in a length of 2.4±0.24 (SD) μm and 5.6±0.72 (SD) μm for the two groups under study. For simplicity, we will refer in the sequel to these groups as the 2- and 5-μm groups. Analysis of the movement of the nanorods following magnetic field-induced rotation discriminated the nanorods that had been internalized by the cells from those that remained in the extracellular milieu. For the region of analysis, the nanorod insertion rate measured as the ratio of the number of nanorods effectively inserted in cells over the number of nanorods deposited in the region was 0.61±0.15 (SD) and 0.29±0.17 (SD), whereas the final number of embedded nanorods per cell for the samples considered in this study is 1.16±0.70 (SD) and 0.44±0.20 (SD) for the 2- and 5-μm groups, respectively. On average, 37% of cells did not absorb 2-μm nanorods and 66% of cells did not absorb 5-μm nanorods. We observed up to six nanorods embedded in one cell for the 2-μm case and up to four nanorods in one cell for the 5-μm case. The embedded nanorods observed in this study were found in the cytoplasm, usually around the perinuclear region with no preferred orientation. This observation is to be expected, because endocytic vesicles are driven by dynein toward the minus end of microtubules, located in the perinuclear region of the cell. No nanorods were observed inside the nucleus.

Rotation of nanorods subjected to a single revolution of magnetic field

Nanorods inside the cytoplasm of cells were capable of deforming internal structures and cellular membranes. Deformation of the nucleus and plasma membrane were readily visible (Figure 2). To study the ability of nanorods to generate intracellular perturbation, their response to magnetic field was quantified in terms of total angular displacement θ defined as the maximum angle obtained between the extreme orientations that the long axis of an individual nanorod acquires in one revolution of the magnetic field [Figure 3(a)]. The total angular displacement for magnetic fields between 20 and 300 mT is shown in Figure 3(b). We found that all rods remained immobile for a magnetic field intensity as high as 20 mT and progressively rotated with increasing field intensity. For both groups of nanorods, the angle θ increased with increasing intensity of the magnetic field; however, the shorter rods tend to attain larger angles than longer rods for a fixed magnetic field intensity. The exposure to one full rotation of the magnetic field did not induce a full rotation of the nanorods and, therefore, θ was less than 360°.

Rotation of nanorods subjected to a rotatory magnetic field

To study the effect of repeated deformation of the intracellular material, nanorods were subjected to a 300 mT rotatory field with a frequency of 10 Hz. Each revolution of the field produced a partial and in some cases full rotation of the nanorods. The corresponding angular displacement was recorded as a function of time. The 2-μm nanorods initially reached an angular displacement of approximately 90° in average and 60% of the nanorods in this group remained at that level after 20 min of exposure to the rotatory field [Figure 5(a)]. The remaining nanorods of the group (40%) underwent full rotation after 10–20 min (Figure 6). In the case of the 5-μm group, no full rotation was observed for any of the nanorods within the 40 min of exposure. The angular displacement remained close to 60° over the entire duration of the test and displayed much less dispersion than the 2-μm nanorod group [Figure 5(b)].

DISCUSSION

In this study, it has been shown that it is possible to obtain low concentrations of embedded nanorods, as low as one nanorod per cell, by direct cell absorption. Based on previous studies,[16] we believe that in our experiments nanorod absorption can be attributed to vesicles that engulf the rods by endocytosis pathways. The insertion rate of the 2-μm nanorods was in general higher than the insertion rate of the 5-μm nanorods, which may turn an important consideration when designing nanoparticles that successfully penetrate into the cytoplasm. The nanorod implantation method used in this work has been analyzed from a toxicity viewpoint, [15] showing that NIH/3T3 cells remain with a normal metabolic activity 24 h after implantation. In our experiments, cells presented a normal cellular and nuclear morphology 24 h after nanorod insertion, showing this method to be less invasive than methods based on ballistic implantation, where a high rate of cell death is found before the application of magnetic fields.[13]

Magnetic nanorods, when free to move in a viscoelastic fluid, follow the orientation of externally applied magnetic fields.[13,17] However, when placed inside the cytoplasm of a

living cell, it was observed that for most cases, motion was restricted and they were not able to fully align in the orientation of the magnetic field. We interpret this restriction as the result of an interaction with firmly anchored cell structures both visible, such as cytoplasmic membrane and nucleus, and nonvisible cellular structures, such as actin filaments.

The null displacement shown by both groups of nanorods for magnetic-field intensities below 20 mT indicates the existence of a minimal torque threshold that needs to be overcome in order for the nanorod to rotate inside the cytoplasm (Figure 3). This result suggests that the cytoplasm of a living cell behaves like a Bingham fluid. Such rheological response is characterized by a yield stress below which no deformation by viscous flow occurs. This behavior has been previously observed in F-actin solutions extracted from a tissue,[18] but to our knowledge, this is the first time being reported inside living cells.

The torque applied on the cell by magnetic nanorods is the consequence of the difference in the orientations of the nanorod magnetic moment and the magnetic field. In nickel nanorods, shape anisotropy predominates over magneto-crystalline anisotropy, rendering their long axis as the energetically favorable direction of magnetization due to high aspect ratio of the particles (length/width). Therefore, the magnetic moment direction of an individual nanorod can be defined by the orientation of its long axis. The torque $\vec{\tau}$ generated by an external magnetic field $\vec{B}$ on a nanorod is given by

$$\vec{\tau} = \vec{\mu} \times \vec{B},$$

where the magnetic dipole moment $\vec{\mu} = \vec{M} \times \vec{V} \times \rho$ is the product of the magnetization $\vec{M}$ (A m^2 kg^{-1}), volume V (m^3) and density ρ (kg m^{-3}) of the material. The magnetization of electrodeposited nickel is similar to the magnetization of bulk nickel at room temperature,[19] that is, 55.4 A m^2 kg^{-1}. Based on the magnetization curve for nickel nanowires measured by Prina-Mello et al., [20] a magnetization of approximately 50 A m^2 kg^{-1} is assumed for the range of magnetic field intensities used in this work. Thus, the magnitudes of the magnetic torque generated by the nickel segments are $\|\vec{\tau}\| = 3.0 \cdot \times 10^{-16}$ Nm and $\|\vec{\tau}\| = 4.5 \times 10^{-15}$ Nm for the 20 and 300 mT fields, respectively. As the nickel segment has the same length for all nanorods used in this study, the induced torque is roughly independent of the nanorod length.

For a 300-mT field, the magnetic torque induces a maximum force of $1.9 \cdot \times 10^{-9}$ and $8.0 \cdot \times 10^{-10}$ N in an average at the edge of the 2- and 5-μm nanorods, respectively. These values are similar to the force necessary for the compression or deformation of a whole cell[21] (up to 10^{-7}–10^{-9} N). Assuming a linear distribution of stress acting on the nanorod and uniform stiffness in the nanorod–cell contact area, the maximum stress at the nanorod tip can be estimated from moment equilibrium as

$$\sigma_{\max} = \frac{6\|\vec{\tau}\|}{dL^2}$$

where *d* and *L* are the diameter and the length of the nanorod, respectively. In consequence, the stress at the nanorod tips is approximately 33.7 and 5.4 kPa for 2- and 5-μm nanorods, respectively. The actin cytoskeleton, which plays a predominant role in the cellular structural strength and cell viscoelastic behavior, has an elastic modulus of around 1 kPa,[22] thus, it is very likely to be deformed by the obtained level of stress. This result is consistent with the observation that nanorods exhibited restricted motion even when they were not obstructed by cellular and nuclear membranes. Presumably, nanorods can deform actin filaments, but they cannot follow the magnetic field for a complete rotation (restricted movement), partly due to actin bundling and crosslinking by actin-binding proteins (ABPs),[23] which increases their stiffness. When in contact with nanorods, we observed that cytoplasmic and nuclear membranes further prevented nanorod motion (Figure 4). It is well known that membrane structures are stiffer than the cytoplasm.[24] A complete mapping of fibroblast stiffness by Plodinec et al. [24] indicates that the cell membrane is the stiffest part of a cell with elastic modulus >10 kPa. The elastic modulus of the nucleus has been found to be 5–8 kPa, about 10 times greater than that of the cytoplasm.[21]

The mechanical response of the two groups of nanorods studied in this work showed important differences when subjected to a rotating magnetic field for several minutes (Figure 5). Between 0 and 40 min of rotational field application, the shorter nanorods showed a marked change in the displacement-angle mean (Welch's *t* test, 10.5 f.d., $p<0.025$), whereas the larger nanorod group did not show a significant change (Welch's t test, 24 f.d., $p \gg 0.025$). Rotation of the 2-μm nanorods is less likely to be limited by the cell membrane or the nucleus because of their shorter length (Figures 4(a, b) and 6). Therefore, the behavior of these nanorods may be predominantly attributed to the interaction with cytoplasmic filaments and other nonvisible structures. In contrast, the rotation of 5-μm nanorods was predominantly prevented by the cytoplasmic and nuclear membranes, structures that are stiffer and more difficult to displace than the cytoplasmic filaments, resulting in smaller rotations [Figures 2, 4(c), and 4(d)].

Rods of same length generate forces of similar magnitude because of the homogeneity of their nickel content, as well as their similar shape and dimensions. Nevertheless, we observed significant variability in the angular displacements of nanorods of the same size (Figures 3 and 5). We attribute this variability to the heterogeneity of the cytoplasm and the different positions and orientations that the nanorods acquired within the cells, as they are heterogeneous and highly anisotropic systems with a complex and variable cytoskeleton structure.[24]

CONCLUSIONS

In this work, the motion of individual Pt-Ni magnetic nanorods embedded in NIH/3T3 fibroblasts and subjected to low-frequency rotatory magnetic fields was studied. None of the nanorods analyzed experienced motion for magnetic torque less than $3.0 \cdot 10^{-16}$ Nm, suggesting a Binghamfluid– type behavior, where a minimum threshold must be overcome to start motion of nanorods and cytoplasmic deformation. Higher intensity magnetic fields produced displacements that disturbed the intracellular environment, generating significant local and global deformation.

The mechanical response of the cell has been extensively studied using several experimental techniques like micropipette aspiration, optical tweezers, and atomic-force microscopy indentation, among others.[25] It should be remarked that these methods involve a strong interaction of the experimental setup with the cellular membrane, making it difficult to directly ascertain cytoplasmic regional properties. Magnetic nanorods as used in this work present a direct and noninvasive method to probe the *in vivo* local mechanical and rheological response of the cytoplasm.

From an application standpoint, the large deformations induced by magnetic nanorods may considerably disrupt internal cell structures, possibly leading to cell damage and death.[11] Therefore, the technique presented in this work may potentially be used in tumor ablation studies. Additionally, the capacity to probe the interior of the cell in a minimally invasive manner can help to elucidate mechanical and structural characteristics of cytoskeleton and organelles.

Acknowledgments

Contract grant sponsor: National Institutes of Health (Fogarty International Center); contract grant number: R03TW008718

References

1. Thiesen B, Jordan A. Clinical applications of magnetic nanoparticles for hyperthermia. Int J Hyperthermia. 2008; 24:467–474. [PubMed: 18608593]
2. Bárcena, C.; Sra, AK.; Gao, J. Applications of magnetic nanoparticles in biomedicine. In: Liu, JP.; Fullerton, E.; Gutfleisch, O.; Sellmyer, DJ., editors. Nanoscale Magnetic Materials and Applications. US: Springer; 2009. p. 591-626.
3. Pankhurst QA, Connolly J, Jones SK, Dobson J. Applications of magnetic nanoparticles in biomedicine. J Phys D Appl Phys. 2003; 36:R167–R181.
4. Hultgren A, Tanase M, Felton EJ, Bhadriraju K, Salem AK, Chen CS, Reich DH. Optimization of yield in magnetic cell separations using nickel nanowires of different lengths. Biotechnol Prog. 2005; 21:509–515. [PubMed: 15801791]
5. Lee IS, Lee N, Park J, Kim BH, Yi YW, Kim T, Kim TK, Lee IH, Paik SR, Hyeon T. Ni/NiO core/shell nanoparticles for selective binding and magnetic separation of histidine-tagged proteins. J Am Chem Soc. 2006; 128:10658–10659. [PubMed: 16910642]
6. Bao J, Chen W, Liu T, Zhu Y, Jin P, Wang L, Liu J, Wei Y, Li Y. Bifunctional Au-Fe3O4 nanoparticles for protein separation. ACS Nano. 2007; 1:293–298. [PubMed: 19206679]
7. Laurent S, Dutz S, Häfeli UO, Mahmoudi M. Magnetic fluid hyperthermia: focus on superparamagnetic iron oxide nanoparticles. Adv Colloid Interface Sci. 2011; 166:8–23. [PubMed: 21601820]
8. Sharma R, Chen CJ. Newer nanoparticles in hyperthermia treatment and thermometry. J Nanopart Res. 2009; 11:671–689.
9. Fortin JP, Gazeau F, Wilhelm C. Intracellular heating of living cells through Néel relaxation of magnetic nanoparticles. Eur Biophys J. 2008; 37:223–228. [PubMed: 17641885]
10. Wilhelm C. Out-of-equilibrium microrheology inside living cells. Phys Rev Lett. 2008; 101:028101-1–4. [PubMed: 18764230]
11. Fung AO, Kapadia V, Pierstorff E, Ho D, Chen Y. Induction of cell death by magnetic actuation of nickel nanowires internalized by fibroblasts. J Phys Chem C. 2008; 112:15085–15088.
12. Jacobs, CR.; Huang, H.; Kwon, RY. Introduction to Cell Mechanics and Mechanobiology. New York: Garland Science; 2013.

13. Celedon A, Hale CM, Wirtz D. Magnetic manipulation of nanorods in the nucleus of living cells. Biophys J. 2011; 101:1880–1886. [PubMed: 22004741]
14. Celedon A, Nodelman IM, Wildt B, Dewan R, Searson P, Wirtz D, Bowman GD, Sun SX. Magnetic tweezers measurement of single molecule torque. Nano Lett. 2009; 9:1720–1725. [PubMed: 19301859]
15. Safi M, Clowez S, Galimard A, Berret JF. In vitro toxicity and uptake of magnetic nanorods. J Phys Conf Ser. 2011; 304:012033.
16. Zhao F, Zhao Y, Liu Y, Chang X, Chen C, Zhao Y. Cellular uptake, intracellular trafficking, and cytotoxicity of nanomaterials. Small. 2011; 7:1322–1337. [PubMed: 21520409]
17. Chen M, Sun L, Bonevich JE, Reich DH, Chien CL, Searson PC. Tuning the response of magnetic suspensions. Appl Phys Lett. 2003; 82:3310–3312.
18. Maruyama K, Kaibara M, Fukada E. Rheology of F-actin I. Network of F-actin in solution Biochim Biophys Acta. 1974; 371:20–29.
19. OReilly C, Sanvito S, Rhen FM, Stamenov P, Coey JMD. Magnetization of electrodeposited nickel: role of interstitial carbon. J Appl Phys. 2006; 99:08J301–08J301.
20. Prina-Mello A, Diao Z, Coey JMD. Internalization of ferromagnetic nanowires by different living cells. J Nanobiotechnol. 2006; 4:9.
21. Caille N, Thoumine O, Tardy Y, Meister JJ. Contribution of the nucleus to the mechanical properties of endothelial cells. J Biomech. 2002; 35:177–187. [PubMed: 11784536]
22. Ananthakrishnan R, Guck J, Wottawah F, Schinkinger S, Lincoln B, Romeyke M, Käs J. Quantifying the contribution of actin networks to the elastic strength of fibroblasts. J Theor Biol. 2006; 242:502–516. [PubMed: 16720032]
23. Gardel ML, Shin JH, MacKintosh FC, Mahadevan L, Matsudaira P, Weitz DA. Elastic behavior of cross-linked and bundled actin networks. Science. 2004; 304:1301–1305. [PubMed: 15166374]
24. Plodinec M, Loparic M, Suetterlin R, Herrmann H, Aebi U, Schoenenberger CA. The nanomechanical properties of rat fibroblasts are modulated by interfering with the vimentin intermediate filament system. J Struct Biol. 2011; 174:476–484. [PubMed: 21426942]
25. Lim CT, Zhou EH, Quek ST. Mechanical models for living cells—a review. J Biomech. 2006; 39:195–216. [PubMed: 16321622]

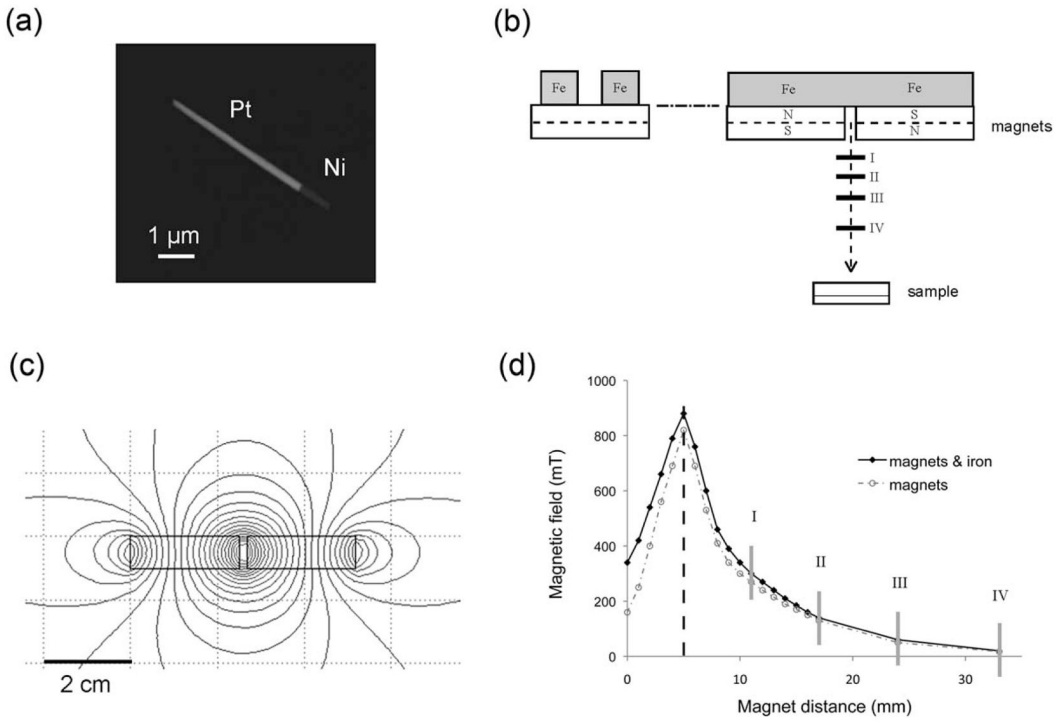

FIGURE 1.

Magnetic nanorods and magnetic manipulators. (a) SEM image of a 5-μm magnetic nanorod. (b) Side and front view of the magnets with iron yokes above. The horizontal solid lines below the magnets represent the different positions where the samples were located. (c) Computer simulation of the magnetic field contours produced by the magnets. (d) Intensity of the magnetic field measured along the central axis [*x*-axis in Figure 1(b)]. Gray vertical lines correspond to the positions where the samples were located.

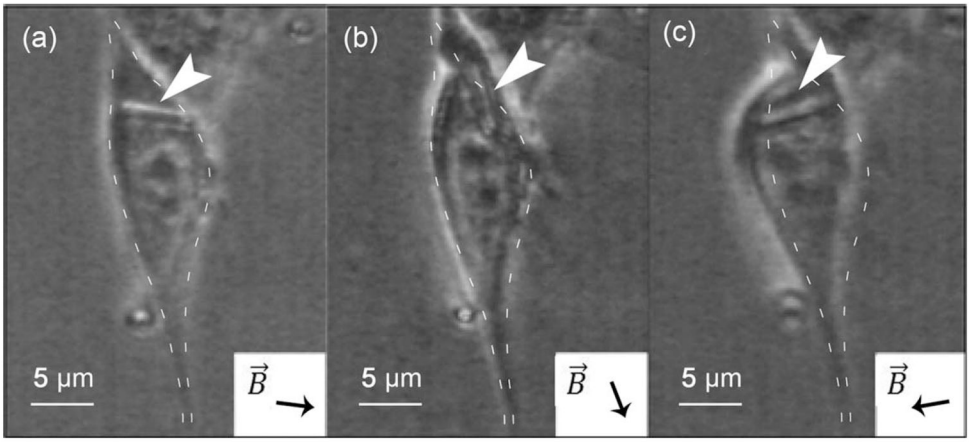

FIGURE 2.

Cell deformation by an externally controlled magnetic nanorod. Deformation of the cell membrane that a single internalized rod is able to generate.

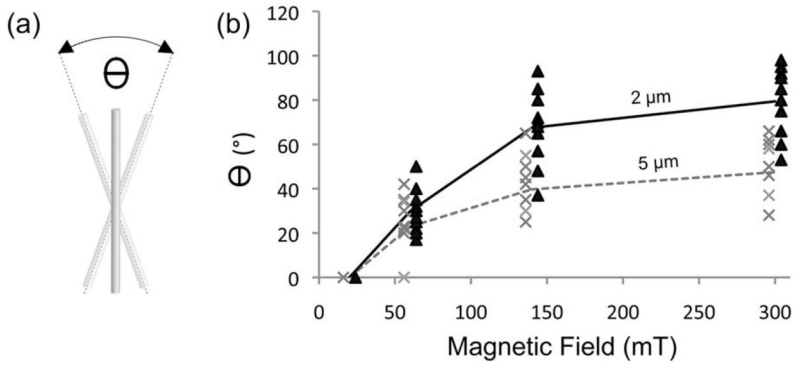

FIGURE 3.

Movement quantification of magnetic nanorods in a live cell. (a) Definition of the total angular displacement θ for an individual nanorod in response to a single revolution of the magnetic field (b) Total angular displacements of 2-μm (black) and 5-μm (gray) nanorods versus magnetic field intensity.

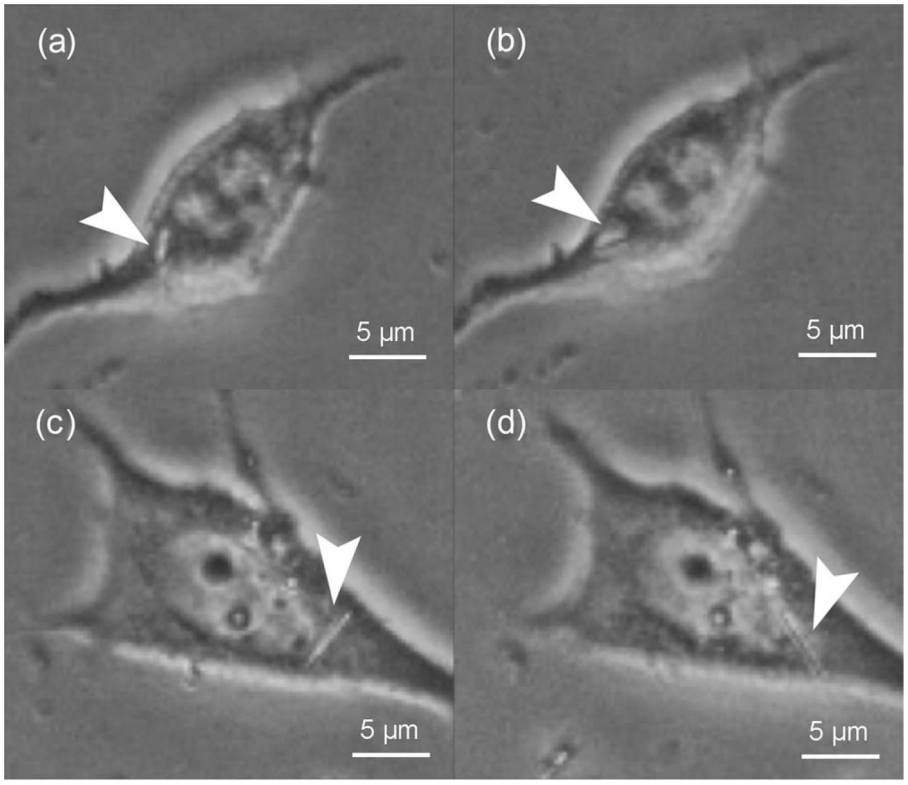

FIGURE 4.

Restricted movement of nanorods during a single magnetic field revolution. Nanorod rotation is restricted by the nucleus and cytoplasmic membrane. (a) and (b) show a 2-μm nanorod, while (c) and (d) show a 5-μm nanorod.

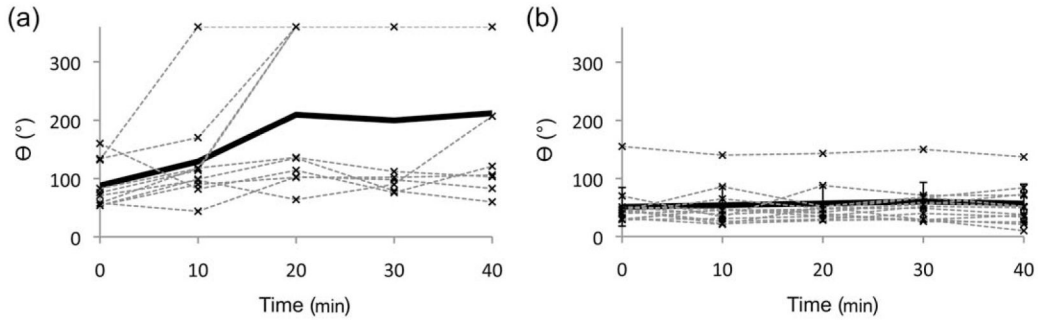

FIGURE 5.

Angular displacement versus time during application of a rotatory 300 mT magnetic field to (a) 2-μm nanorods and (b) 5-μm nanorods. The bold line represents the mean value of all measurements.

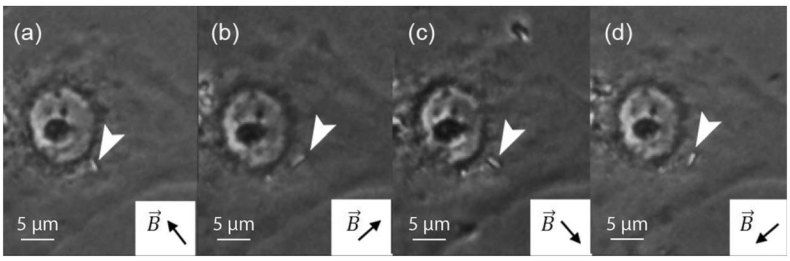

FIGURE 6.

Complete rotation of a 2-μm nanorod following the external magnetic field orientation. (a) to (d) correspond to the magnetic field direction $\vec{B}$ indicated.